ACS ORGANIC & INORGANIC Au
AN OPEN ACCESS JOURNAL OF THE AMERICAN CHEMICAL SOCIETY

Editors' Choice
Open Access

pubs.acs.org/orginorgau

Article

Gold(I)-Catalyzed 1,6-Enyne Single-Cleavage Rearrangements: The Complete Picture

Eduardo García-Padilla, Feliu Maseras,* and Antonio M. Echavarren*

Cite This: *ACS Org. Inorg. Au* 2023, 3, 312−320

Read Online

ACCESS | Metrics & More | Article Recommendations | Supporting Information

ABSTRACT: We identify the factors that rule the selectivity in single-cleavage skeletal rearrangements promoted by gold(I) catalysts. We find that stereoconvergence is enabled by a rotational equilibrium when electron-rich substituents are used. The anomalous *Z*-selective skeletal rearrangement is found to be due to electronic factors, whereas *endo*-selectivity depends on both steric and electronic factors.

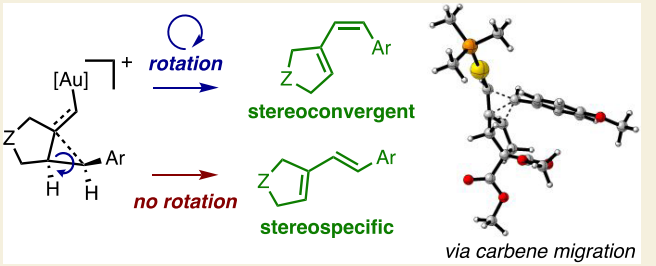

KEYWORDS: *gold carbenes, enynes, rearrangements, metal carbenes, cycloisomerization, DFT mechanistic study*

INTRODUCTION

Due to its high affinity for alkynes, gold(I) complexes have been extensively studied in the cycloisomerization of alkyne-containing substrates.[1−5] Among these cycloisomerizations, gold(I)-catalyzed skeletal rearrangements of 1,*n*-enynes cleave at least one of the carbon−carbon bonds and lead to structural diversity.[6,7] In principle, both exocyclic or endocyclic single-cleavage and double-cleavage rearrangements can occur, leading to a variety of distinct potential diene products for a given substrate.[8,9] In the case of 1,6-enynes, the initial η^2-alkyne gold(I) complex **1** can form bicyclic gold(I) carbene **2**, which can undergo a single-cleavage rearrangement to form *exo*-type 1,3-diene **3** and/or *endo*-type 1,3-diene **4** (Scheme 1a).[7−13] Alternatively, a double-cleavage rearrangement of **2** can lead to new gold(I) carbene intermediate **5** by formal insertion of the terminal carbon of the alkene into the alkyne triple bond (Scheme 1). Gold(I) carbene **5** can undergo α-proton elimination to give rise to 1,3-dienes of type **6**.

The *exo*-type versus *endo*-type single-cleavage rearrangement leading to products **3** or **4** depends on the substitution of the double bond of 1,6-enynes, as well as on the nature of the tether. Thus, for example, 1,6-enynes **7a** and **7b** give rise to *exo*-type products **8a** and **8b**, whereas **7c** preferentially affords six-membered ring *endo*-type product **9**.[8,9,13]

Prior to the discovery that gold(I) complexes were highly active and selective for the skeletal rearrangement of 1,6-enynes,[8,9] complexes of ruthenium(II),[14] platinum(II)[15−17] platinum(IV),[18] rhodium(II),[19] iridium(I),[20] as well as Lewis acids $GaCl_3$[21] and $InCl_3$,[22−24] were studied. While most substrates undergo these transformations preferentially, seemingly minor changes in the substrate, catalyst, or solvent have important effects on the selectivity.[8,25−29]

In general, metal-catalyzed rearrangement of 1,6-enynes proceeding by single-cleavage is stereospecific. (Scheme 2a).[14] The stereospecific rearrangements of ***E***- and ***Z***-**7d** into ***E***- and ***Z***-**8d**, respectively, promoted by $GaCl_3$[21] and the gold(I)-catalyzed conversions of ***E***-**7e** into ***E***-**8e** and ***Z***-**7f** into ***Z***-**8f**[8,9] illustrate this general trend (Scheme 1a). However, in an early example catalyzed by ruthenium(II), both *E*- and *Z*-configured **7e** gave the most stable *E*-isomer of **8e**.[14] Similar formation of the *E*-isomer from both *E*- and *Z*-configured 1,6-enynes was observed in the rhodium(II)-catalyzed[19] transformation.

We observed a more surprising exception in the gold(I)-catalyzed skeletal rearrangement of some 1,6-enynes that were found to form the less stable *Z*-isomers (Scheme 2b).[30] Thus, for example, 1,6-enynes ***E***-**7g** and ***E***-**7h** with electron-donating substituents at the alkene (cyclopropyl and *p*-$MeOC_6H_4$) underwent a selective skeletal rearrangement to give thermodynamically less favorable products ***Z***-**8g** and ***Z***-**8h**. The rearrangement of the *Z*-configured 1,6-enynes also afforded *Z*-configured products, in a stereoconvergent manner. It is interesting to note, that, in contrast, the iridium(I)-catalyzed rearrangement of the diethyl malonate analogue of ***E***-**7g** provides exclusively the *E*-configured 1,3-diene.[20]

In this study, we investigate the factors that contribute to the anomalous *Z*-selective skeletal rearrangement using computational methods to gain insights into the underlying mechanisms. In addition, we explore the steric and electronic effects on the

Received: June 28, 2023
Revised: July 28, 2023
Accepted: July 31, 2023
Published: August 20, 2023

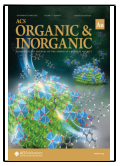

Scheme 1. (a) Single versus Double Skeletal Rearrangement of 1,6-Enynes. (b) Tether Dependence on *exo*- and *endo*-Selectivity

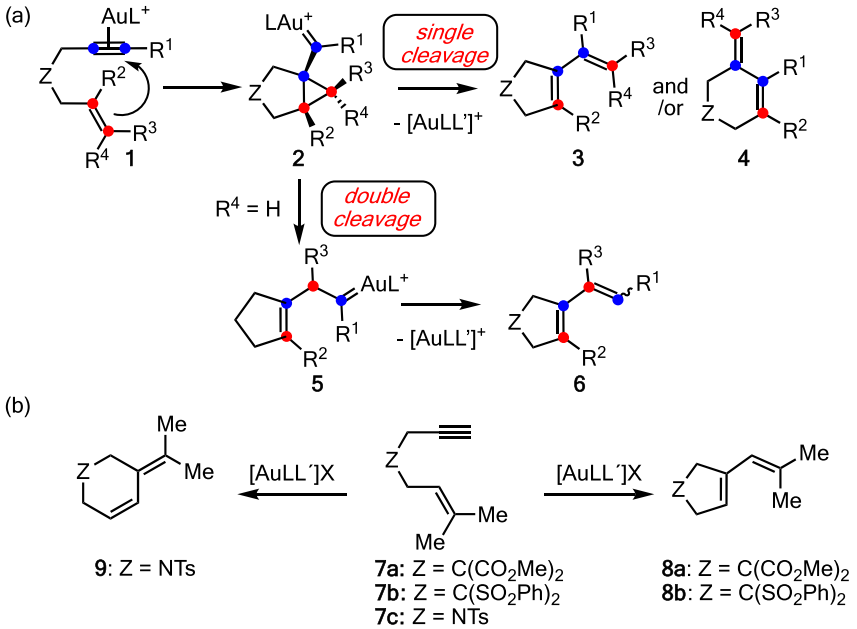

Scheme 2. (a) Examples of *E*-Selective or Stereospecific Single-Cleavage Skeletal Rearrangement and (b) Abnormal *Z*-Selective Single-Cleavage Skeletal Rearrangement

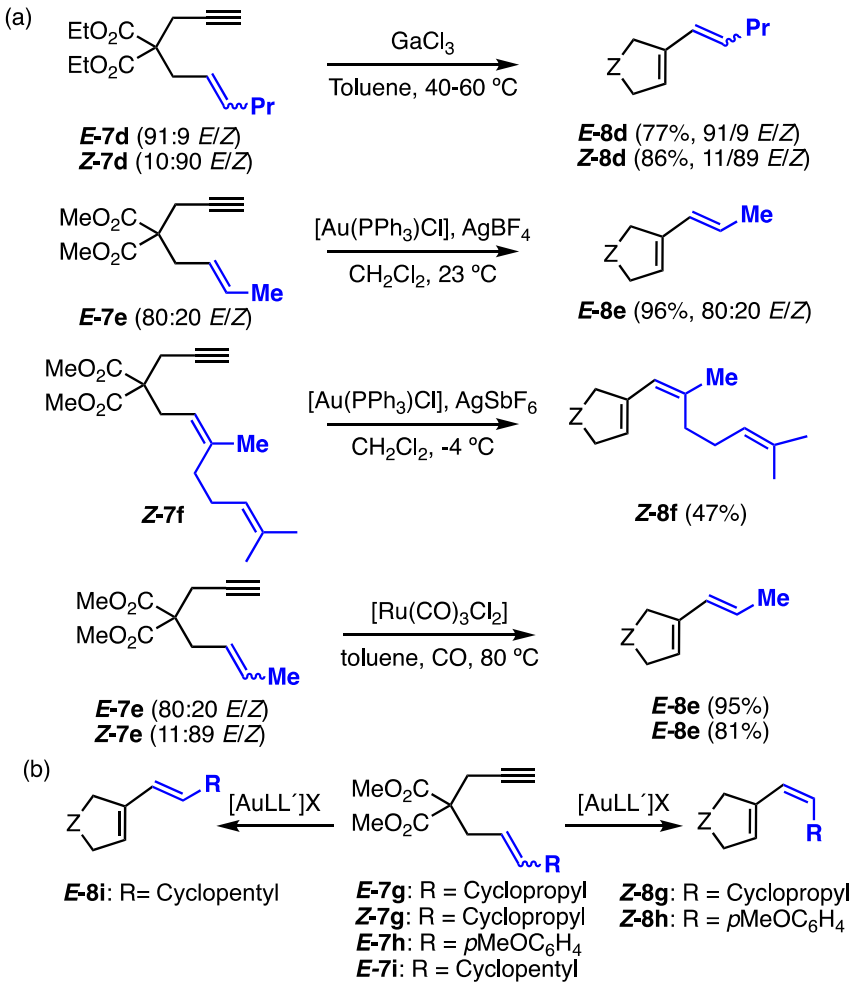

https://doi.org/10.1021/acsorginorgau.3c00028
ACS Org. Inorg. Au 2023, 3, 312−320

Scheme 3. (a–f) Gold(I)-Catalyzed 1,6-Enyne Single-Cleavage Skeletal Rearrangements

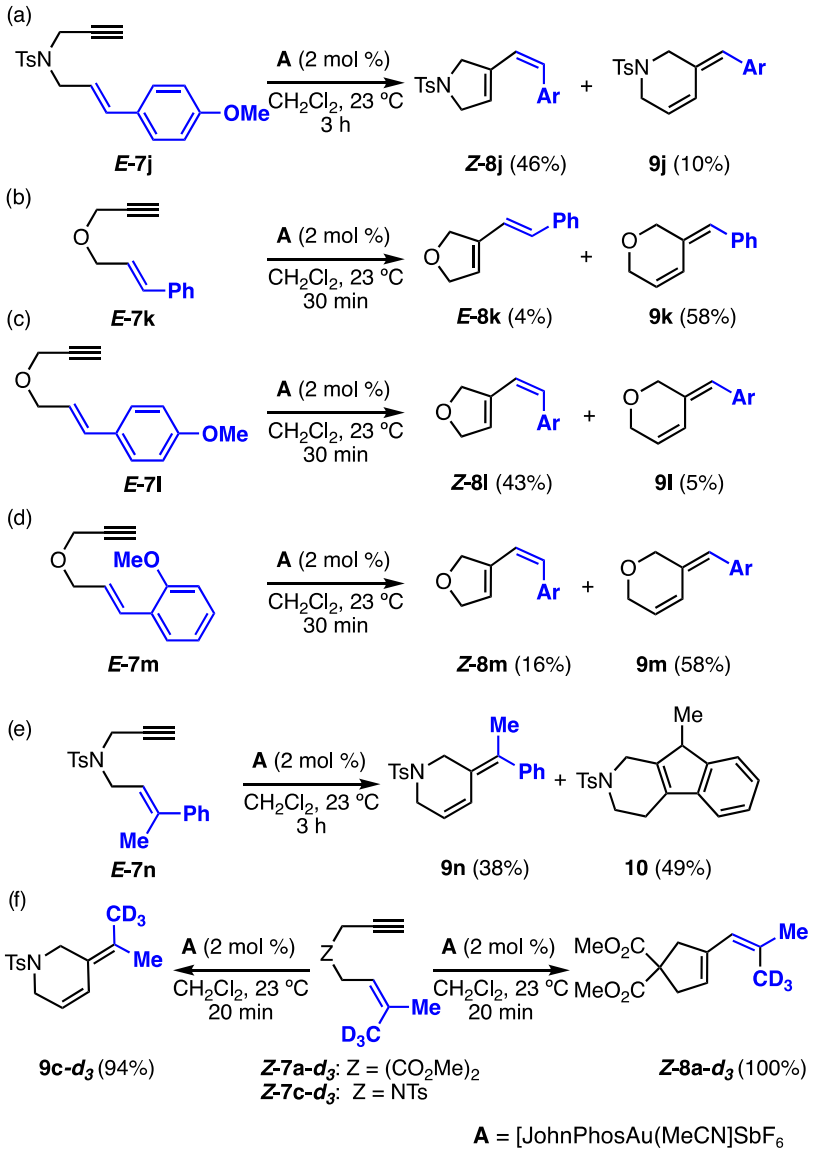

exo-type or *endo*-type single-cleavage rearrangement and whether the latter *endo*-type could also lead to products in a stereoconvergent manner.

RESULTS AND DISCUSSION

As the *N*-sulfonamide tether was known to increase selectivity for the *endo*-cleavage product in gold(I)-catalyzed skeletal rearrangements of 1,6-enynes,[8,9] substrate ***E*-7j** with an electron-rich alkene and the *N*-sulfonamide tether was synthesized (Scheme 3a). The reaction of ***E*-7j** with commercially available [JohnPhosAu(MeCN)]SbF_6 (**A**) led to ***Z*-8** as the major product, along with small amounts of *endo*-type product **9j**. On the other hand, whereas cinnamyl propargyl ether (***E*-7k**) led to small amounts of ***E*-8k** together with *endo*-type **9k** as the major product (Scheme 3b), both ***E*-7l** and ***E*-7m** with more electron-rich *p*- and *o*-methoxyphenyl groups, afforded ***Z*-8l** and ***Z*-8m**, together with *endo*-type products **9l** and **9m**, respectively (Scheme 3c,d). 1,6-Enyne ***E*-7n**, with a trisubstituted alkene, gave *endo*-type **9n** and tricyclic derivative **10**, which is presumably formed in the Nazarov-type cyclization of **9n** (Scheme 3e).

We also synthesized two 1,6-enynes ***Z*-7a-d_3** and ***Z*-7c-d_3** bearing Me and CD_3 at the terminal carbon of the alkene as well as different tethers to confirm the stereospecificity of the gold(I)-catalyzed single-cleavage rearrangements (Scheme 3d). Thus, ***Z*-7a-d_3** reacted in the presence of catalyst **A** to give *exo*-type ***Z*-8a-d_3** in quantitative yield, and *endo*-type ***Z*-7c-d_3** gave **9a-d_3** in 94% yield. Although the two different types of single-cleavage rearrangements were observed depending on the tether, both reactions took place with full retention of the configuration at the alkene.

With the aim of explaining all these observations, we carried out density functional theory (DFT) calculations. The B3LYP-D3 functional was used with implicit dichloromethane solvation.[31] Unless otherwise specified, trimethylphosphine gold(I) was used as a model for the catalyst in most of the computational work, as Buchwald phosphines, triaryl phosphites, and NHC ligands all showed similar behavior experimentally.[30]

The mechanism for the *exo*-single-cleavage rearrangement was explored first (Scheme 4). 1,6-Enynes ***E*-7h** and ***Z*-7h** with a strongly electron-donating *p*-methoxyphenyl group at the alkene

https://doi.org/10.1021/acsorginorgau.3c00028
ACS Org. Inorg. Au 2023, 3, 312–320

Scheme 4. Mechanism of the Gold(I)-Catalyzed *Z*-Selective *exo*-Single-Cleavage Skeletal Rearrangement of *E*-7h and *Z*-7h[a]

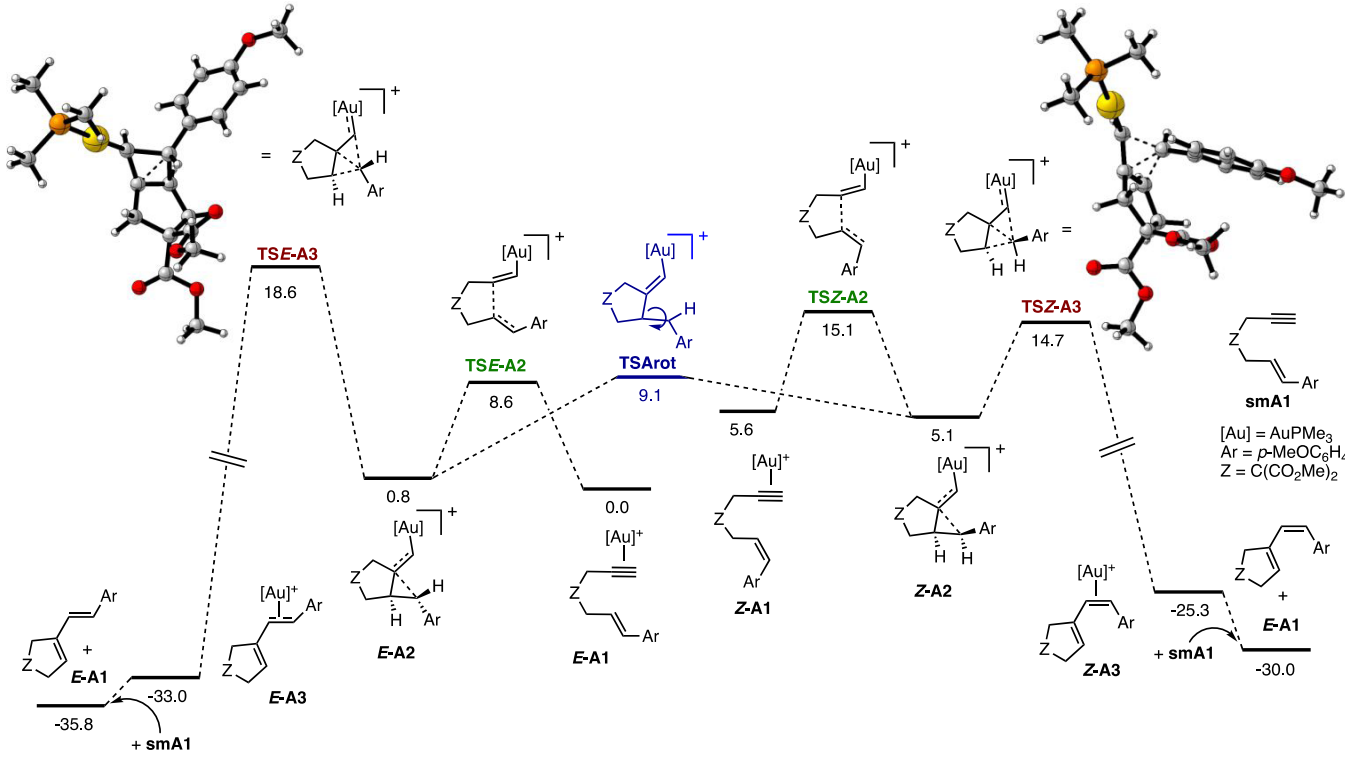

[a]Free energy in kcal/mol.

were chosen as the substrates, and their corresponding gold(I) complexes ***E*-A1** and ***Z*-A1** were the reference points in the reaction coordinate (Scheme 4). The *exo*-cyclization of ***E*-A1** and ***Z*-A1** give cyclopropyl gold(I) carbenes ***E*-A2** and ***Z*-A2**, respectively, through transition states **TS*E*-A2** and **TS*Z*-A2**. Although ***E*-A2** is significantly more stable than ***Z*-A2**, its rearrangement to give ***E*-A3** proceeds through **TS*E*-A3**, which is 3.9 kcal/mol higher than **TS*Z*-A3**, leading to ***Z*-A3**. The direct *E*/*Z* isomerization of the alkene is not feasible, but ***E*-A2** and ***Z*-A2** are in equilibrium through accessible transition state **TSArot** (9.1 kcal/mol), which has lower energy than **TS*E*-A3** and **TS*Z*-A3** (18.6 and 14.7 kcal/mol, respectively). Therefore, the most favorable pathway from either ***E*-A1** or ***Z*-A1** takes place via ***Z*-A2** and **TS*Z*-A3** to finally give rise to ***Z*-A1**, in agreement with the experimental results (Scheme 2b).[30]

The rearrangement through **TS*Z*-A3** (or **TS*E*-A3**) is a concerted 1,3-migration of the ArCH fragment across an allyl π system (Figure 1). This single-cleavage skeletal rearrangement can therefore be described as a suprafacial 1,3-sigmatropic shift of an sp^2 carbon. The distances between the migrating carbene ArCH fragment and the allyl cation carbons (all 1.70−1.71 Å) suggest significant backdonation into the π system. Bicyclobutonium cations are in fact known in the context of non-classical carbocationic species.[32] However, in this case, the bicyclobutonium form would correspond to a transition state and not as a minimum in the reaction coordinate.

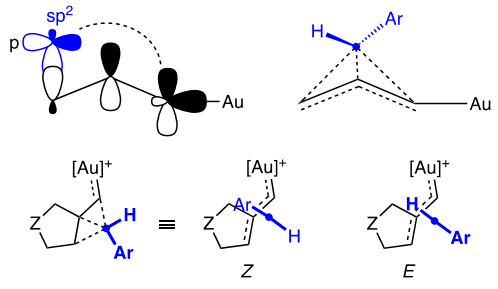

Figure 1. Model for the 1,3-sigmatropic shift in the transition state as a formal cyclobutonium cation. Cleavage of the single bond results in a carbene migrating across an allyl cation.

Alternative mechanisms to that presented in Scheme 4 could be envisaged, but we found them to be non-competitive.[31] A possibility would be the involvement of cyclobutene intermediates and subsequent gold(I)-catalyzed ring opening.[10,33] While some [4,5]-fused cyclobutenes are known in cycloisomerizations,[34−36] the reaction coordinate for their formation would be very similar to that of the single cleavage. This leads to the presence of a substrate-dependent bifurcation.[33] In this case, there is no transition state connecting gold(I) α-cyclopropyl carbene ***E*-A2** to bicyclo[3.2.0]heptane **A4** (Scheme 5). A retro-scan from fused cyclobutene **A4** to the starting material only gave **A5** (Scheme 5), which is not formed from ***E*-A1** (Scheme 4). Therefore, the involvement of bicyclo[3.2.0]heptenes is discarded for the studied terminal 1,6-enynes. Due to the partial double bond nature of the C1−C2 bond in ***E*-A2**, the barrier to

Scheme 5. Formation of Bicyclo[3.2.0]heptenes is Not Feasible from These Substrates

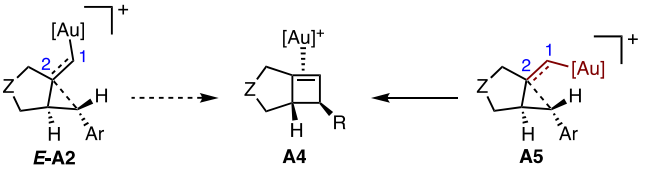

https://doi.org/10.1021/acsorginorgau.3c00028
ACS Org. Inorg. Au 2023, 3, 312−320

Scheme 6. Model Showing Competition between Internal Rotation and *exo*-Migration of Different Enynes Using [JohnPhosAu] as a Catalyst

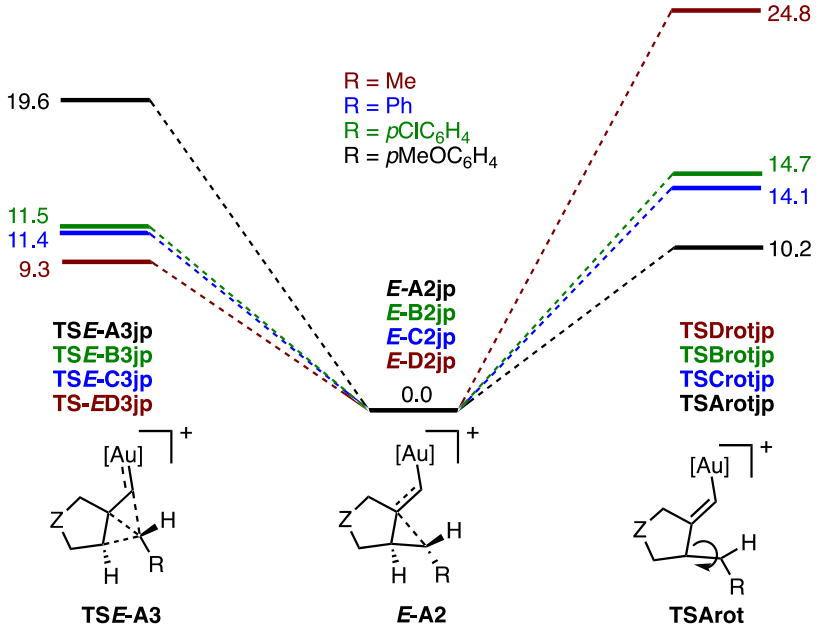

formation of the cyclobutene would be comparable to that of rotation around the double bond.[37]

For alkenes with strongly electron-donating substituents, this barrier through transition states similar to **TSArot** between the *E*- and *Z*-cyclopropyl gold(I) carbenes, such as ***E*-A2** and ***Z*-A2** in Scheme 4, is significantly lower than the rearrangement transition states. The phenyl and *p*-chlorophenyl analogue substrates were calculated to probe the influence of the electronics on the stereoselectivity. The experimentally observed fall in *Z*-selectivity for less electron-rich substrates could arise either from the inversion in energy barriers, favoring the *E*-product instead, or from a sufficient increase in energy in the torsional barriers such that the system is no longer under equilibrium conditions and becomes stereospecific. This is in line with the experimental results of **Z-7a-d_3**, which forms the product stereospecifically, whereas any interconverting pathway would show isomerization to a 1:1 ratio. While the full mechanisms were calculated with trimethylphosphine, a model of the *E*-migration and rotation was calculated with JohnPhos while freezing the structure of the atoms in the substrate.[31] The results predict the shift from stereospecific to *Z*-stereoconvergent reactions (Scheme 6).

The relative barriers of the *Z*- and *E*-migration TS are 2.5 kcal mol^{-1} in the case of cinnamyl (R = Ph) and even higher for *p*-Cl ($\Delta\Delta G^{\ddagger}$ = 4.1 kcal mol^{-1}) and *p*-MeO ($\Delta\Delta G^{\ddagger}$ = 3.9 kcal mol^{-1}) substrates. The calculation of the torsional energy barriers showed that these were greatly affected by the electronics on the ring. Less electron-donating substituents on the alkene would lead to stereospecific transformations.

As our calculations fully reproduce the experimental behavior, we then sought to explain the reasons for the selectivity. The barrier to rotation is defined by the α-cyclopropyl carbene character of the intermediate in which the presence of electron-rich stabilizing groups such as aryl or cyclopropyl groups lowers the barrier to a greater extent than electron-poor aryl or methyl groups.

The explanation for the electronic stabilization of the *Z*-transition state is not trivial, as the delocalization of the aromatic ring electron density into the migrating carbon empty orbital should not be greatly affected by the configuration. Resorting to the bicyclobutonium complex model, the selectivity may then be reformulated as "the *Z*-configuration favors η^3 coordination of the allyl fragment".

NBO analysis was performed on the optimized *Z* and *E* transition state geometries on the smaller model molecule. The NBO second-order perturbation analysis shows that in *Z*-TS (**TSZ-E3**), there is much more delocalization of the formal C1−C7 and C6−C7 σ bond NBOs to the C2 empty orbital, accounting for a stabilization of 64 kcal mol^{-1} of the bicyclobutonium structure (Figure 2). Moreover, there are several weaker stabilizing interactions that account for a small further increase in *cis* stabilization.[31]

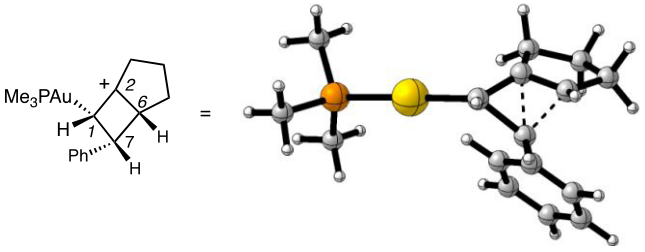

Figure 2. Lewis structure of the transition state used in NBO analysis and 3D rendition showing the bicyclobutonium geometry.

The charges of the Me_3PAu (*E* and *Z* = +1.13) and benzylidene fragments (*E* = +0.17, *Z* = +0.18) are very similar in both transition states. For this reason, the preference for the *Z*-migration cannot arise from a change in the localization of benzylic charge, as both isomers would be too similar in this respect.

However, the resonance onto the allyl system is very different according to the second-order perturbation analysis. This corresponds to the stabilization of the η^3-like allyl−carbene system for *Z*-TS relative to that of *E*-TS. This result, in turn, arises from the better overlap in aromatic $\pi \rightarrow \sigma^*$ donation,

https://doi.org/10.1021/acsorginorgau.3c00028
ACS Org. Inorg. Au 2023, 3, 312−320

which is geometrically more accessible for the *Z*-isomer. Therefore, the *Z*-configuration weakens the C1−C7 and C6−C7 σ bond character of the migrating carbene by allowing π backdonation, lowering the energy of the bicyclobutonium geometry. For this explanation to be correct, the *E*-isomer should show a worse overlap between the C2 p orbital and the σ bonds to C7. This is confirmed by the NBO charge of C2 being slightly higher for the *E*-isomer (E = +0.24, Z = +0.15), implying less delocalized C1−C7 and C6−C7 bonds. Similar substituent effects on the stability of bicyclobutonium cations, albeit as intermediates, were reported in the solvolysis of substituted cyclobutyl methanesulfonates.[38]

We also carried out calculations of the transition state for the 1,3-migration substituting the malonate tether by CH_2 or CMe_2, and comparable energies were found in all cases (Table 1). This shows that the difference in energy is not governed by supramolecular interactions with the tether.

Table 1. $\Delta\Delta G^{\ddagger}$ between the *E*- or *Z*-1,3-Migration for a Cinnamyl Propargyl Substrate with Different Tethers Using $Me_3PAu(I)$

entry	Z tether	$\Delta\Delta G^{\ddagger}$ (kcal/mol)
1	$C(CO_2Me)_2$	2.6
2	CH_2	2.9
3	CMe_2	2.9

The *endo*-type single-cleavage skeletal rearrangement leads to six-membered ring products by 5-*exo*-dig cyclization. 1,6-Enynes with *N*-sulfonamide tethers or with less electron-rich alkenes favor the *endo*-type skeletal rearrangement instead of the most common *exo*-type single-cleavage.[8,9,13] Using *N*-*p*-methoxycinnamyl-*N*-propargylmethanesulfonamide as a model for substrate ***E*-7j** (Scheme 3a), we have investigated computationally the stereospecificity of this rearrangement as well as the causes of the selectivity between *exo*-type and *endo*-type cleavage (Scheme 7).

We used ***E*-F1** and ***Z*-F1** (shown in the Supporting Information) as the origin of the mechanism. They cyclize analogously to ***E*-A1** and ***Z*-A1** to form ***E*-F2** and ***Z*-F2**, respectively, and the transition state corresponding to the bond rotation was located. As had been observed with the malonate tether, **TSF1rot** was energetically accessible and lower in energy than either **TS*E*-F3** or **TS*Z*-F4**, which led to products (Scheme 7). The *exo*-cleavage transition states **TS*Z*-F3** and **TS*E*-F3** also showed a +2.4 kcal/mol preference for the *Z* pathway, leading to ***Z*-F3**. In fact, of all four possible products, ***Z*-F3** would be the major product predicted by DFT, which fully reproduces the experimental results in the preferential formation of ***Z*-8j** (Scheme 3a).

The *endo*-cleavage products would form in a two-step process, first involving the migration of the *endo*-carbene in **TS*E*-F4** and **TS*Z*-F4** to form intermediate cyclopropyl gold intermediates ***E*-**

Scheme 7. Mechanism of the Gold(I)-Catalyzed *exo*- and *endo*-Single-Cleavage Skeletal Rearrangements of *N*-Propargyl-*N*-(*p*-methoxycinnamyl)methanesulfonamide[a,b]

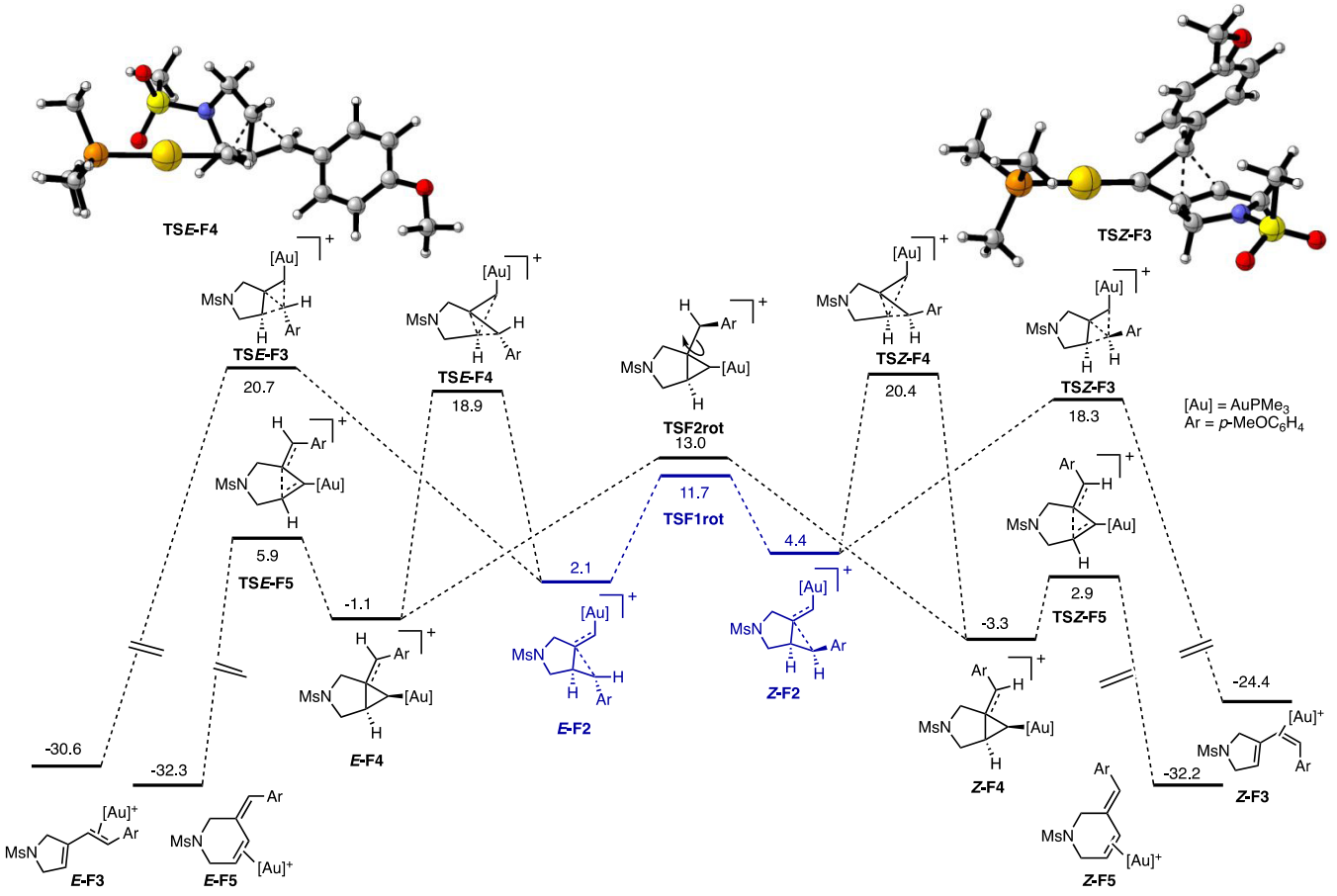

[a]Free energy in kcal/mol. [b]Formation of the initial gold(I) cyclopropyl carbene (blue) can be found in the Supporting Information.

https://doi.org/10.1021/acsorginorgau.3c00028
ACS Org. Inorg. Au 2023, 3, 312−320

F4 and ***Z*-F4**, respectively. This cyclopropyl gold intermediate would form the six-membered ring product via concerted asynchronous ring opening and change in hapticity after **TS*E*-F5** and **TS*Z*-F5**. Notably, even though there is a transition state **TSF2rot** that can connect both precursors ***E*-F4** and ***Z*-F4** by C−C bond rotation, this transition state is too high in energy to compete with either **TS*E*-F5** or **TS*Z*-F5**, so any stereoconvergence in the *endo*-type products must arise from **TSF1rot**. These calculations also reproduce the formation of the second product, **9j** (Scheme 3a), in approximately the observed experimental ratio.

While the energy profile above reproduces the experimental data, the factors deciding the *exo*- and *endo*-type pathways, and why electron-donating substituents switch the selectivity, remained to be explained. We sought to explain both observations, as the *Z*-selectivity of the *exo*-cleavage mechanism is analogous to that observed in all previous mechanisms. Transition states **TS*E*-F4** and **TS*Z*-F4**, the rate-limiting steps leading to the *endo*-type cleavage products, each has a fully formed bond to the benzylic carbon. On the other hand, *exo*-type cleavage transition states **TS*E*-F3** and **TS*Z*-F3** both require a partial cleavage thereof. As electron-rich substituents lead to intermediates with a higher vinyl gold carbocation character, this results in the *exo*-type cleavage being more favorable, as the corresponding bond is weakened. For intermediates with a higher cyclopropyl carbene character, the *endo*-type cleavage is more accessible. This explains the increase in formation of the *exo*-type product for very electron-rich alkenes.

In addition, and when comparing substrates with the same alkenes in the *endo*-type cleavage, the cyclopropyl gold(I) intermediates formed upon migration result in LAu facing *endo* with respect to the bicyclic system. This may explain why more sterically hindered tethers can favor the *exo*-type selectivity, whereas a sulfonamide or an ether can point away from the catalyst and facilitate *endo*-type cleavage. This is consistent with the general trend seen experimentally for cinnamyl and prenyl substrates (Scheme 3b,e,f).

CONCLUSIONS

The *Z*-selectivity of the single-cleavage skeletal rearrangement of 1,6-enynes is influenced by two primary factors: the ability to access an equilibrium scenario between *E*- and *Z*-configured cyclopropyl gold(I) carbenes and the electronic preference for *Z*-migration of the most electron-rich substituent. Electron-rich substituents on the alkene allow the interconversion between the *Z*- and *E*-isomers by rotation, which explains the *Z*-selective stereoconvergent process. The *Z*-selectivity is purely electronic and is independent of the catalyst. This is significant, as it would mean carbene-type migrations have intrinsic electronic preferences.

Less sterically hindered tethers can favor the *endo*-cleavage pathways, but sufficiently electron-rich alkenes will still undergo the analogous *Z*-selective *exo*-type cleavage. Stereoconvergence in the *endo*-cleavage products could in principle also take place but would be more difficult to observe, as the same factors that lead to loss of stereospecificity also contribute to favoring exocyclic migrations.

METHODS

General Procedure for the Cycloisomerization of 1,6-Enynes

To a stirred solution of enyne (400 μmol) in CH_2Cl_2 (4 mL) at 23 °C was added [JohnPhosAu(NCMe)]SbF_6 (8.0 μmol, 2 mol %). After stirring for the given time, the reaction was quenched with a drop of triethylamine, and the solution was concentrated in vacuo. The crude product was purified by column chromatography on silica or neutral alumina.

Computational Methods

All calculations were carried out on Gaussian09. The geometry optimizations of the complexes were performed with B3LYP using Grimme's D3 dispersion correction with the 6-31G(d) basis set for non-metal atoms and the SDD basis set and ECP for gold. Single-point energy calculations were performed with the 6-311+G(d,p) basis set for non-metal atoms and the SDD basis set and ECP for gold. The implicit polarizable continuum model (PCM) for dichloromethane was used in all calculations, and the cationic complexes were modeled with the exclusion of the counteranions. All stationary points were verified by the absence of imaginary vibrations and transition states confirmed by IRC calculations. The transition states for the hindered rotations were confirmed with IRC relaxation with Hratchian and Schlegel's damped velocity Verlet algorithm (DVV). The reported free energies were calculated at 298 K and 1 atm. NBO analysis was performed with the NBO3.0 program with B3LYP-D3, the 6-311+G(d,p) basis set for non-metal atoms and the SDD basis set and ECP for gold.

ASSOCIATED CONTENT

Data Availability Statement

The computational data underlying this study are openly available in the ioChem-BD repository at https://doi.org/10.19061/iochem-bd-1-287.[39]

Supporting Information

The Supporting Information is available free of charge at https://pubs.acs.org/doi/10.1021/acsorginorgau.3c00028.

Procedures; characterization; NMR spectra; and DFT computations (PDF)

AUTHOR INFORMATION

Corresponding Authors

Feliu Maseras − *Institute of Chemical Research of Catalonia (ICIQ-CERCA), The Barcelona Institute of Science and Technology, 43007 Tarragona, Spain; Departament de Química Analítica i Química Orgànica, Universitat Rovira i Virgili, 43007 Tarragona, Spain;* orcid.org/0000-0001-8806-2019; Email: fmaseras@iciq.es

Antonio M. Echavarren − *Institute of Chemical Research of Catalonia (ICIQ-CERCA), The Barcelona Institute of Science and Technology, 43007 Tarragona, Spain; Departament de Química Analítica i Química Orgànica, Universitat Rovira i Virgili, 43007 Tarragona, Spain;* orcid.org/0000-0001-6808-3007; Email: aechavarren@iciq.es

Author

Eduardo García-Padilla − *Institute of Chemical Research of Catalonia (ICIQ-CERCA), The Barcelona Institute of Science and Technology, 43007 Tarragona, Spain; Departament de Química Analítica i Química Orgànica, Universitat Rovira i Virgili, 43007 Tarragona, Spain*

Complete contact information is available at: https://pubs.acs.org/10.1021/acsorginorgau.3c00028

https://doi.org/10.1021/acsorginorgau.3c00028
ACS Org. Inorg. Au 2023, 3, 312−320

Author Contributions

CRediT: **Eduardo García-Padilla** investigation (equal).

Notes

The authors declare no competing financial interest.

■ ACKNOWLEDGMENTS

The authors thank the MCIN/AEI/10.13039/501100011033 (PID2019-104815GB-I00, PID2020-112825RB-I00, and CEX2019-000925-S), the European Research Council (Advanced Grant 835080), the AGAUR (2021 SGR 01256 and predoctoral fellowship to EG-P (2020FI_B 00403)), and CERCA Program/Generalitat de Catalunya for financial support. The authors also thank the ICIQ X-ray diffraction, NMR, and chromatography and mass spectrometry units.

■ REFERENCES

(1) Hashmi, A. S. K. Homogeneous gold catalysts and alkynes: A successful liaison. *Gold Bull.* **2003**, *36*, 3−9.
(2) Fürstner, A.; Davies, P. W. Catalytic Carbophilic Activation: Catalysis by Platinum and Gold π Acids. *Angew. Chem., Int. Ed.* **2007**, *46*, 3410−3449.
(3) Jiménez-Núñez, E.; Echavarren, A. M. Gold-Catalyzed Cycloisomerizations of Enynes: A Mechanistic Perspective. *Chem. Rev.* **2008**, *108*, 3326−3350.
(4) Obradors, C.; Echavarren, A. M. Gold-Catalyzed Rearrangements and Beyond. *Acc. Chem. Res.* **2014**, *47*, 902−912.
(5) Fensterbank, L.; Malacria, M. Molecular Complexity from Polyunsaturated Substrates: The Gold Catalysis Approach. *Acc. Chem. Res.* **2014**, *47*, 953−965.
(6) Zhang, L.; Sun, J.; Kozmin, S. A. Gold and platinum catalysis of enyne cycloisomerization. *Adv. Synth. Catal.* **2006**, *348*, 2271−2296.
(7) Dorel, R.; Echavarren, A. M. Gold(I)-Catalyzed Activation of Alkynes for the Construction of Molecular Complexity. *Chem. Rev.* **2015**, *115*, 9028−9072.
(8) Nieto-Oberhuber, C.; Muñoz, M. P.; Buñuel, E.; Nevado, C.; Cárdenas, D. J.; Echavarren, A. M. Cationic Gold(I) Complexes: Highly Alkynophylic Catalysts for the Exo- and Endo-Cyclization of Enynes. *Angew. Chem., Int. Ed.* **2004**, *43*, 2402−2406.
(9) Nieto-Oberhuber, C.; Muñoz, M. P.; López, S.; Jiménez-Núñez, E.; Nevado, C.; Herrero-Gómez, E.; Raducan, M.; Echavarren, A. M. Gold(I)-Catalyzed Cyclizations of 1,6-Enynes: Alkoxycyclizations and Exo/Endo Skeletal Rearrangements. *Chem. - Eur. J.* **2006**, *12*, 1677−1693.
(10) Escribano-Cuesta, A.; Pérez-Galán, P.; Herrero-Gómez, E.; Sekine, M.; Braga, A. A. C.; Maseras, F.; Echavarren, A. M. The Role of Cyclobutenes in Gold(I)-Catalysed Skeletal Rearrangement of 1,6-Enynes. *Org. Biomol. Chem.* **2012**, *10*, 6105−6111.
(11) Ferrer, C.; Raducan, M.; Nevado, C.; Claverie, C. K.; Echavarren, A. M. Missing Cyclization Pathways and New Rearrangements Unveiled in the Gold(I) and Platinum(II)-Catalyzed Cyclization of 1,6-Enynes. *Tetrahedron* **2007**, *63*, 6306−6316.
(12) Soriano, E.; Marco-Contelles, J. Mechanistic Insights on the Cycloisomerization of Polyunsaturated Precursors Catalyzed by Platinum and Gold Complexes. *Acc. Chem. Res.* **2009**, *42*, 1026−1036.
(13) Cabello, N.; Jiménez-Núñez, E.; Buñuel, E.; Cárdenas, D. J.; Echavarren, A. M. On the Mechanism of the Puzzling "Endocyclic" Skeletal Rearrangement of 1,6-Enynes. *Eur. J. Org. Chem.* **2007**, 4217−4223.
(14) Chatani, N.; Morimoto, T.; Muto, T.; Murai, S. Highly Selective Skeletal Reorganization of 1,6- and 1,7-Enynes to 1-Vinylcycloalkenes Catalyzed by $RuCH_2(CO)_3$. *J. Am. Chem. Soc.* **1994**, *116*, 6049−6050.
(15) Chatani, N.; Furukawa, N.; Sakurai, H.; Murai, S. $PtCl_2$-Catalyzed Conversion of 1,6- and 1,7-Enynes to 1-Vinylcycloalkenes. Anomalous Bond Connection in Skeletal Reorganization of Enynes. *Organometallics* **1996**, *15*, 901−903.
(16) Fürstner, A.; Szillat, H.; Stelzer, F. Novel Rearrangements of Enynes Catalyzed by $PtCl_2$. *J. Am. Chem. Soc.* **2000**, *122*, 6785−6786.
(17) Oi, S.; Tsukamoto, I.; Miyano, S.; Inoue, Y. Cationic Platinum-Complex-Catalyzed Skeletal Reorganization of Enynes. *Organometallics* **2001**, *20*, 3704−3709.
(18) Oh, C. H.; Bang, S. Y.; Rhim, C. Y. PtCl4-catalyzed Cycloreorganization of 1,6- and 1,7-Enynes. *Bull. Korean Chem. Soc.* **2003**, *24*, 887−888.
(19) Ota, K.; Lee, S. I.; Tang, J.-M.; Takachi, M.; Nakai, H.; Morimoto, T.; Sakurai, H.; Kataoka, K.; Chatani, N. Rh(II)-Catalyzed Skeletal Reorganization of 1,6- and 1,7-Enynes through Electrophilic Activation of Alkynes. *J. Am. Chem. Soc.* **2009**, *131*, 15203−15211.
(20) Inoue, H.; Morimoto, T.; Muto, T.; Murai, S.; Chatani, N. Indium(I)-Catalyzed Cycloisomerization of Enynes. *J. Org. Chem.* **2001**, *66*, 4433−4436.
(21) Chatani, N.; Inoue, H.; Kotsuma, T.; Murai, S. Skeletal Reorganization of Enynes to 1-Vinylcycloalkanes. *J. Am. Chem. Soc.* **2002**, *124*, 10294−10295.
(22) Miyanohana, Y.; Chatani, N. Skeletal Reorganization of Enynes Catalyzed by $InCl_3$. *Org. Lett.* **2006**, *8*, 2155−2158.
(23) Zhuo, L.-G.; Zhang, J.-J.; Yu, Z.-X. DFT and Experimental Exploration of the Mechanism of $InCl_3$ -Catalyzed Type II Cycloisomerization of 1,6-Enynes: Identifying $InCl_2$+ as the Catalytic Species and Answering Why Nonconjugated Dienes Are Generated. *J. Org. Chem.* **2012**, *77*, 8527−8540.
(24) Zhuo, L.-G.; Zhang, J.-J.; Yu, Z.-X. Mechanisms of the $InCl_3$-Catalyzed Type-I, II, and III Cycloisomerizations of 1,6-Enynes. *J. Org. Chem.* **2014**, *79*, 3809−3820.
(25) Kim, N.; Brooner, R. E. M.; Widenhoefer, R. A. Unexpected Skeletal Rearrangement in the Gold(I)/Silver(I)-Catalyzed Conversion of 7-Aryl-1,6-Enynes to Bicyclo[3.2.0]Hept-6-Enes via Hidden Brønsted Acid Catalysis. *Organometallics* **2017**, *36*, 673−678.
(26) Gagosz, F. Unusual Gold(I)-Catalyzed Isomerization of 3-Hydroxylated 1,5-Enynes: Highly Substrate-Dependent Reaction Manifolds. *Org. Lett.* **2005**, *7*, 4129−4132.
(27) Muratov, K.; Gagosz, F. Confinement-Induced Selectivities in Gold(I) Catalysis-The Benefit of Using Bulky Tri-(*ortho* -biaryl)-phosphine Ligands. *Angew. Chem., Int. Ed.* **2022**, *61*, No. e20220345.
(28) Chen, G.-Q.; Fang, W.; Wei, Y.; Tang, X.-Y.; Shi, M. Divergent Reaction Pathways in Gold-Catalyzed Cycloisomerization of 1,5-Enynes Containing a Cyclopropane Ring: Dramatic Ortho Substituent and Temperature Effects. *Chem. Sci.* **2016**, *7*, 4318−4328.
(29) Calleja, P.; Pablo, Ó.; Ranieri, B.; Gaydou, M.; Pitaval, A.; Moreno, M.; Raducan, M.; Echavarren, A. M. α,β-Unsaturated Gold(I) Carbenes by Tandem Cyclization and 1,5-Alkoxy Migration of 1,6-Enynes: Mechanisms and Applications. *Chem. - Eur. J.* **2016**, *22*, 13613−13618.
(30) Jiménez-Núñez, E.; Claverie, C. K.; Bour, C.; Cárdenas, D. J.; Echavarren, A. M. Cis -Selective Single-Cleavage Skeletal Rearrangement of 1,6-Enynes Reveals the Multifaceted Character of the Intermediates in Metal-Catalyzed Cycloisomerizations. *Angew. Chem., Int. Ed.* **2008**, *47*, 7892−7895.
(31) See Supporting Information for additional details
(32) Staral, J. S.; Yavari, I.; Roberts, J. D.; Surya Prakash, G. K.; Donovan, D. J.; Olah, G. A. Low-temperature carbon-13 nuclear magnetic resonance spectroscopic investigation of C_4H_7+. Evidence for an equilibrium involving the nonclassical bicyclobutonium ion and the bisected cyclopropylcarbinyl cation. *J. Am. Chem. Soc.* **1978**, *100*, 8016−8018.
(33) Odabachian, Y.; Gagosz, F. Cyclobutenes as Isolable Intermediates in the Gold(I)-Catalysed Cycloisomerisation of 1,8-Enynes. *Adv. Synth. Catal.* **2009**, *351*, 379−386.
(34) Buisine, O.; Aubert, C.; Malacria, M. Cobalt(I)-Mediated Cycloisomerization of Enynes: Mechanistic Insights. *Chem. - Eur. J.* **2001**, *7*, 3517−3525.
(35) Brooner, R. E. M.; Brown, T. J.; Widenhoefer, R. A. Direct Observation of a Cationic Gold(I)-Bicyclo[3.2.0]Hept-1(7)-Ene Complex Generated in the Cycloisomerization of a 7-Phenyl-1,6-Enyne. *Angew. Chem., Int. Ed.* **2013**, *52*, 6259−6261.

https://doi.org/10.1021/acsorginorgau.3c00028
ACS Org. Inorg. Au 2023, 3, 312−320

(36) Brooner, R. E. M.; Robertson, B. D.; Widenhoefer, R. A. Mechanism of 1,3-Hydrogen Migration in a Gold Bicyclo[3.2.0]-Heptene Complex: The Role of Brønsted Acid in the Gold-Catalyzed Cycloisomerization of 7-Aryl-1,6-Enynes. *Organometallics* **2014**, *33*, 6466−6473.
(37) Nieto-Oberhuber, C.; López, S.; Muñoz, M. P.; Cárdenas, D. J.; Buñuel, E.; Nevado, C.; Echavarren, A. M. Divergent Mechanisms for the Skeletal Rearrangement and [2+2] Cycloaddition of Enynes Catalyzed by Gold. *Angew. Chem., Int. Ed.* **2005**, *44*, 6146−6148.
(38) Creary, X. 3-*t*-Butyl-1-methylcyclobutyl Cation. Experimental vs Computational Insights into Tertiary Bicyclobutonium Cations. *J. Org. Chem.* **2020**, *85*, 7086−7096.
(39) Álvarez-Moreno, M.; de Graaf, C.; Lopez, N.; Maseras, F.; Poblet, J. M.; Bo, C. Managing the Computational Chemistry Big Data Problem: The ioChem-BD Platform. *J. Chem. Inf. Model.* **2015**, *55*, 95−103.

https://doi.org/10.1021/acsorginorgau.3c00028
ACS Org. Inorg. Au 2023, 3, 312−320